J|A|C|S ARTICLES

Published on Web 07/15/2010

Electrochemical Behavior and Electrogenerated Chemiluminescence of Star-Shaped D−A Compounds with a 1,3,5-Triazine Core and Substituted Fluorene Arms

Khalid M. Omer,[†] Sung-Yu Ku,[†,‡] Yu-Chen Chen,[‡] Ken-Tsung Wong,*[,‡] and Allen J. Bard*[,†]

Center for Electrochemistry, Department of Chemistry and Biochemistry, University of Texas at Austin, Austin, Texas 78712, and Department of Chemistry, National Taiwan University, 106 Taipei, Taiwan

Received May 14, 2010; E-mail: ajbard@mail.utexas.edu; kenwong@ntu.edu.tw

Abstract: We report the synthesis, electrochemistry, and electrogenerated chemiluminescence of a series of star-shaped donor−acceptor (D−A) molecules. The star-shaped molecules consist of an electron-deficient 1,3,5-triazine core with three fluorene arms substituted with diarylamino (**TAM1**−**TAM3**) or carbazolyl (**TAM4**) electron donors. Cyclic voltammetry of **TAM1**−**TAM3** shows that the reduction consists of one wave of single electron transfer to the core, while the oxidation exhibits a single peak of three sequential electron-transfer processes, with the formation of a trication. The carbazole-containing molecule **TAM4** after oxidation undergoes a subsequent rapid chemical reaction to produce a dimer (via the overall coupling of two radical cations with the loss of two protons). The dimer electrooxidizes more easily than the monomer of **TAM4**. With continuous cycling on the oxidation side, a conductive polymer film is formed on the surface of the working electrode. Because of the presence of the acceptor (triazine) center and strong donors in the arms (diarylamine or carbazole), **TAM1**−**TAM3** exhibit large solvatochromic effects with emissions ranging from deep blue (428 nm) to orange-red (575 nm) depending on the solvent polarity. These star-shaped molecules show high PL quantum yields of 0.70−0.81. The electrogenerated chemiluminescence (ECL) of **TAM1**−**TAM3** in nonaqueous solutions showed strong ECL that could be seen with the naked eye in a well-lit room. Because the enthalpy of annihilation is higher than the energy required for formation of the singlet excited state, the ECL emission is believed to be generated via S-route annihilation. However, **TAM4** shows weak annihilation ECL because of the production of polymer film on the electrode surface during oxidation cycles. However, by limiting the potential region only to the reduction side and using benzoyl peroxide (BPO) as a coreactant, strong ECL of **TAM4** can be obtained.

Introduction

In the present work, we report the synthesis, electrochemical, and photochemical characterization and electrogenerated chemiluminescence of star-shaped molecules based on a 1,3,5-triazine core with three arms built with 9,9-diethylfluorene end-capped with diarylamine or carbazole, as shown in Figure 1. Star-shaped donor-π-acceptor (D-A) systems are considered promising candidates for different applications, such as organic light-emitting devices,[1] photovoltaic applications,[2] and organic thin film transistors.[3]

Recently, we reported blue electrogenerated chemiluminescence (ECL) of star-shaped molecules based on truxene−oligofluorene.[4] The truxene−oligofluorene compounds show *C*3 symmetry; however, in the hydrocarbon structure, there were no strong D and A groups to stabilize the hole or the electron, i.e., to stabilize the radical cation and anion. Therefore, we designed and synthesized a *C*3 symmetry system by introducing strong donor groups (diarylamine for **TAM1**−**TAM3** or car-

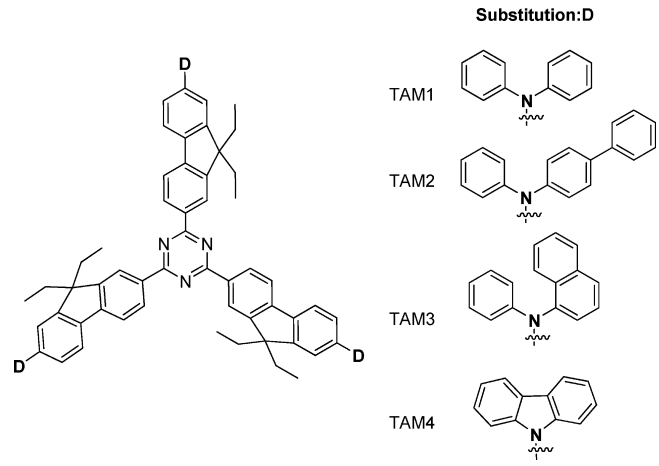

Figure 1. Star-shaped 1,3,5-triazine derivatives.

[†] University of Texas at Austin.
[‡] National Taiwan University.

(1) (a) Lai, W.-Y.; He, Q.-Y.; Zhu, R.; Chen, Q.-Q.; Huang, W. *Adv. Funct. Mater.* **2008**, *18*, 265. (b) Xu, T.; Lu, R.; Liu, X.; Chen, P.; Qiu, X.; Zhao, Y. *J. Org. Chem.* **2008**, *73*, 1809. (c) Kreger, K.; Bäte, M.; Neuber, C.; Schmidt, H.-W.; Strohriegl, P. *Adv. Funct. Mater.* **2007**, *17*, 3456. (d) Zhou, X-.H.; Yan, J.-C.; Pei, J. *Org. Lett.* **2003**, *5*, 3543. (e) Wu, I.-Y.; Lin, J. T.; Tao, Y.-T.; Balasubramaniam, E.; Su, Y. Z.; Ko, C.-W. *Chem. Mater.* **2001**, *13*, 2626.
(2) (a) Cremer, J.; Bauerle, P. *J. Mater. Chem.* **2006**, *16*, 874. (b) Roquet, S.; Cravino, A.; Leriche, P.; Ale'veque, O.; Fre're, P.; Roncali, J. *J. Am. Chem. Soc.* **2006**, *128*, 3459. (c) Thelakkat, M. *Macromol. Mater. Eng.* **2002**, *287*, 442.

 10.1021/ja104160f

Scheme 1. Electrooxidation of Triphenylamine and Following Dimerization of Triphenylamine

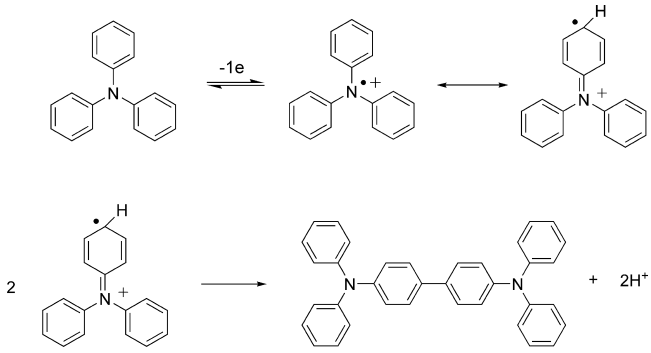

bazole for **TAM4**) and the strong electron acceptor (1,3,5-triazine) bridged by the 2,7-fluorenes. Diarylamine or carbazole with lone pair electrons on the nitrogen makes these derivatives easy to oxidize. Shirota et al.[5] designed various systems of star-shaped triarylamine-based molecules, which have different effects on lowering the potential for oxidation based on their conjugation lengths. Unsubstituted triphenylamine (TPA) undergoes dimerization to form tetraphenylbenzidine as shown by ESR and cyclic voltammetry (Scheme 1).[6] The dimer is oxidized more easily than the monomer of TPA.

1,3,5-Triazine molecules show good optical and electrochemical properties.[7] Due to their electron deficiency (i.e., triazine is a typical acceptor unit), radical anions are stabilized, and reduction occurs reversibly. Such radical anion stability is a fundamental requirement of generating efficient ECL.

Electrogenerated chemiluminescence (ECL) arises from the electron transfer between a cation radical and an anion radical.[8] The simplest ECL mechanism is the direct annihilation reaction between the cation radical and the anion radical as follows:

$$A - e \rightarrow A^{\bullet +} \text{ (radical cation formation)} \quad (1)$$

$$A + e \rightarrow A^{\bullet -} \text{ (radical anion formation)} \quad (2)$$

$$A^{\bullet -} + A^{\bullet +} \rightarrow {}^1A^* + A \text{ (singlet state formation by direct annihilation)} \quad (3)$$

$${}^1A^* \rightarrow A + h\nu \text{ (ECL emission)} \quad (4)$$

However, asymmetric annihilation, for example between a dianion and monocation may occur to produce the excited state by the following two proposed mechanisms:[9]

Mechanism I:

$$A^{\bullet -}-D-A^{\bullet -} + A-D^{\bullet +}-A \rightarrow A^{\bullet -}-D-A + (A-D-A)^* \quad (5)$$

$$A^{\bullet -}-D-A + A - D^{\bullet +}-A \rightarrow A-D-A + (A-D-A)^* \quad (6)$$

Mechanism II:

$$A^{\bullet -}-D - A^{\bullet -} + A-D-A \rightarrow 2A^{\bullet -}-D-A \quad (7)$$

$$A^{\bullet -}-D-A + A-D^{\bullet +}-A \rightarrow A-D-A + (A-D-A)^* \quad (8)$$

However, in the presence of strong acceptor and donor, an intramolecular charge-transfer emission is possible as radical anion and radical cation collide.

$$A^{\bullet -}-D-A^{\bullet -} + A-D^{\bullet +}-A \rightarrow (A^{\bullet -}-D^{\bullet +}-A)^* + A-D-A \quad (9)$$

$$(A^{\bullet -}-D^{\bullet +}-A)^* \rightarrow A-D-A + h\nu \quad (10)$$

Another ECL pathway, often used when lack of stability of one radical ion or the limitation of the potential window to prevent its generation, involves adding a coreactant, which can produce either a strong reducing agent or strong oxidizing agent depending on the nature of the coreactant. For example, benzoyl peroxide (BPO) is one of the common coreactants used if the radical cation is not stable. Upon reduction, BPO forms a strong oxidizing agent ($E^\circ = +1.5$ V),[10] which can directly react with an anion to produce an excited state.

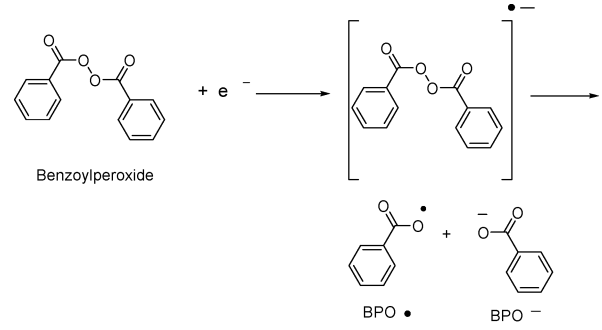

(11)

$$BPO^{\bullet} + A^{\bullet -} \rightarrow A^* + BPO^- \quad (12)$$

$$A^* \rightarrow A + h\nu \quad (13)$$

D−A molecules are sensitive to solvent polarity, due to the intramolecular charge transfer that occurs upon excitation. As a result, they are potential solvent polarity probes.[11]

In this paper, we describe the synthesis of **TAM1**−**TAM4**. Electrochemistry and spectroscopy are thoroughly studied. **TAM1**−**TAM3** show bright ECL, which could be seen with the naked eye under ambient light.

Experimental Section

Synthesis. TAM1−**TAM4** consist of a 1,3,5-triazine core and three arms of 9,9-diethylfluorene end-capped with diarylamine or carbazole. The syntheses of **TAM1**−**TAM4** start from 2-bromo-9,9-diethylfluorene to give 2-cyano-9,9-diethylfluorene, followed by an acid-promoted triazene formation and C−N bond cross-coupling reaction. This synthetic route was shown in Scheme 2. Treatment of 2-bromo-9,9-diethylfluorene[12] with 2 equiv of CuCN

(3) (a) Kim, K. H.; Chi, Z.; Cho, M. J.; Jin, J.-I.; Cho, M. Y.; Kim, S. J.; Joo, J.-S.; Choi, D. H. *Chem. Mater.* **2007**, *19*, 4925. (b) Ponomarenko, S. A.; Tatarinova, E. A.; Muzafarov, A. M.; Kirchmeyer, S.; Brassat, L.; Mourran, A.; Moeller, M.; Setayesh, S.; De Leeuw, D. *Chem. Mater.* **2006**, *18*, 4101. (c) Horowitz, G. *Adv. Mater.* **1998**, *10*, 365.
(4) Omer, K. M.; Kanibolotsky, A. L.; Skabara, P. J.; Perepichka, I. F.; Bard, A. J. *J. Phys. Chem. B* **2007**, *111*, 6612.
(5) (a) Shirota, Y.; Kageyama, H. *Chem. Rev.* **2007**, *107*, 953. (b) Shirota, Y. *J. Mater. Chem.* **2005**, *15*, 75. (c) Shirota, Y. *J. Mater. Chem.* **2000**, *10*, 1.
(6) (a) Nelson, R. F.; Adams, R. N. *J. Am. Chem. Soc.* **1968**, *90*, 3925. (b) Seo, E. T.; Nelson, R. F.; Fritsch, J. M.; Marcoux, L. S.; Leedy, D. W.; Adams, E. N. *J. Am. Chem. Soc.* **1966**, *88*, 3498.
(7) (a) Fang, Q.; Yamamoto, T. *Macromol. Chem. Phys.* **2004**, *205*, 795. (b) Cui, Y. Z.; Fang, Q.; Lei, H.; Xue, G.; Yu, W. T. *Chem. Phys. Lett.* **2003**, *377*, 507. (c) Pang, J.; Tao, Y.; Freiberg, S.; Yang, X.-P.; D'Iorio, M.; Wang, S. *J. Mater. Chem.* **2002**, *12*, 206. (d) Cherioux, F.; Audebert, P.; Hapiot, P. *Chem. Mater.* **1998**, *10*, 1984. (e) Fink, R.; Frenz, C.; Thelakkat, M.; Schmidt, H.-W. *Macromolecules* **1997**, *30*, 8177.

Scheme 2. Synthetic Pathway of **TAM** Compounds

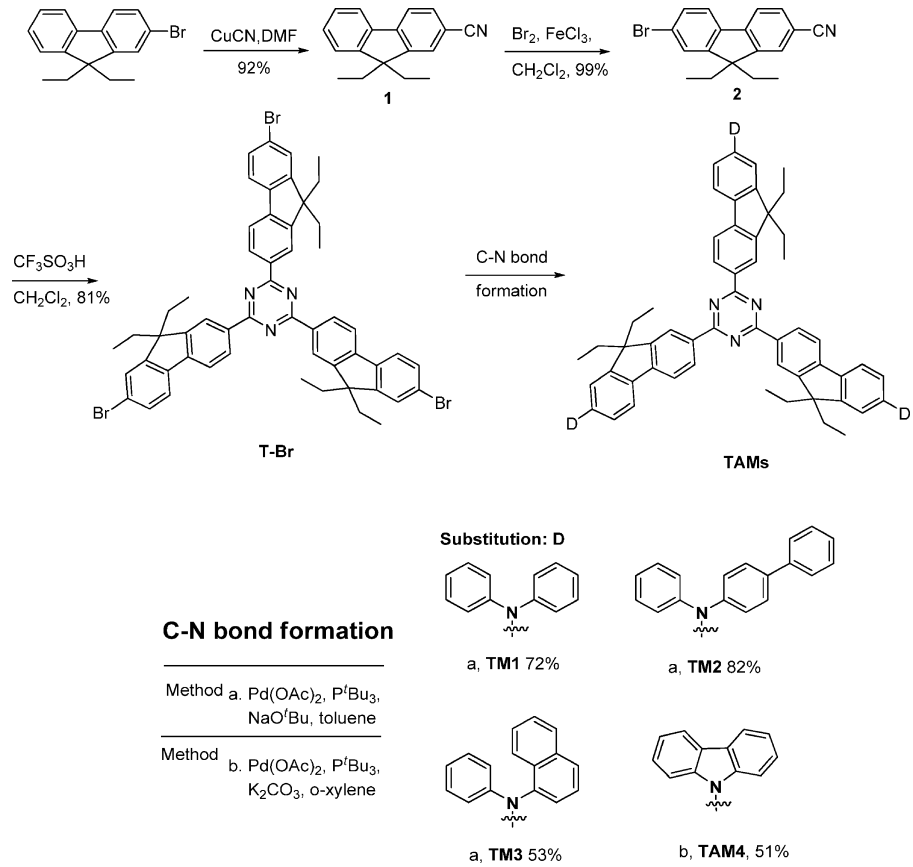

in DMF at reflux temperature gave 2-cyano-9,9-diethylfluorene (compound **1**) in an isolated yield of 92%. Compound **1** was regioselectively brominated at C-7 with 2 equiv of bromine in the presence of Lewis acid ($FeCl_3$) to give compound **2** in 99%. Then, CF_3SO_3H-promoted cyclization of compound **2** in dichloromethane generated 1,3,5-triazine **T-Br** in an isolated yield of 81%. Finally, Pd-catalyzed C−N bond formation of **T-Br** with a different diarylamine using NaO^{t}Bu as base at 110 °C afforded **TAM1**−**TAM3**. The same procedure was not feasible for the C−N bond coupling with carbazole substitution. K_2CO_3 was employed as base, instead of NaO^{t}Bu. The mixture was stirred at 160 °C in *o*-xylene in the presence of $Pd(OAc)_2$ and P^{t}Bu$_3$ generated the **TAM4** in a moderate yield.

Compound 2. Compound **1** (9.8 g, 40 mmol) was dissolved in chloroform (20 mL), and the mixture was lined with aluminum foil to keep away from light. Then bromine (4 mL, 80 mmol) was added slowly into the flask, and the reaction mixture was stirred at the reflux temperature for 12 h. The mixture was extracted with $CHCl_3$/water. The organic solution was collected, dried with $MgSO_4$, and concentrated with a rotary evaporator. The product was purified by vacuum system to get compound **2** as a brown solid: (13.0 g, 99%). mp 95−96 °C; IR (KBr) ν 2979, 2230, 1607, 1448, 824, 519 cm^{-1}; ^{1}H NMR ($CDCl_3$, 400 MHz) δ 7.74 (d, J = 8.0 Hz, 1H), 7.66−7.59 (m, 3H), 7.53−7.50 (m, 2H), 2.05−1.99 (m, 4H) 0.29 (t, J = 7.4 Hz, 6H); ^{13}C NMR ($CDCl_3$, 100 MHz) δ 152.5, 150.0, 144.7, 138.3, 131.3, 130.4, 126.4, 126.3, 123.0, 121.9, 120.1, 119.4, 110.3, 56.8, 32.5, 8.4; MS (*m*/*z*, FAB$^+$) 326 (52), 307 (18), 217 (24), 154 (100), 136 (77); HRMS ((M + H)$^+$, FAB$^+$) Calcd $C_{18}H_{17}{}^{79}BrN$ 326.0544, found 326.0545; calcd $C_{18}H_{17}{}^{81}BrN$ 328.0524, found 328.0533. Anal. Calcd C, 66.27; H, 4.94; Br, 24.49; N, 4.29; found C, 66.49; H, 4.95; N, 4.03.

TBr. Compound **2** (12.8 g, 40 mmol) and trifluoromethanesulfonic acid (3.6 mL, 40 mmol) were dissolved in dichloromethane (40 mL). The reaction mixture was stirred at 0 °C for 1 h and then stirred at room temperature for 24 h. The mixture was extracted with CH_2Cl_2/water. The organic solution was collected and dried with $MgSO_4$, and the organic solvents were removed with a rotary evaporator. The product was purified by recrystallization with methanol to get **T-Br** as a white solid: (10.4 g, 81%). mp 214 °C (DSC); IR (KBr) ν 2979, 1613, 1593, 1249, 811, 751 cm^{-1}; ^{1}H NMR ($CDCl_3$, 400 MHz) δ 8.86 (dd, J = 8.0, 1.6 Hz, 3H), 8,74 (d, J = 0.8 Hz, 3H), 7.91 (d, J = 8.0 Hz, 3H), 7.70 (d, J = 7.6 Hz, 3H), 7.56 −7.53 (m, 6H), 2.29−2.24 (m, 6H), 2.16−2.10 (m, 6H), 0.435 (t, J = 7.4 Hz, 18H); ^{13}C NMR ($CDCl_3$, 100 MHz) δ 171.5, 153.1, 149.8, 144.8, 139.6, 135.4, 130.2, 128.5, 126.4, 123.2, 122.2, 121.7, 119.8, 56.7, 32.8, 8.6; MS (*m*/*z*, FAB$^+$) 980 (43), 978 (43), 326 (24), 307 (60), 289 (52); HRMS ((M + H)$^+$, FAB$^+$) Calcd $C_{54}H_{49}N_3{}^{79}Br^{81}Br_2$ 980.1436, found 980.1433; calcd $C_{54}H_{49}N_3{}^{79}Br_2{}^{81}Br$ 978.1456, found 978.1460.

TAM1. $Pd(OAc)_2$ (23 mg, 0.1 mmol), diphenylamine (700 mg, 4 mmol), Na^{t}BuO (460 mg, 6 mmol), and **T-Br** (980 mg, 1 mmol) were added to a 100 mL two-neck flask with a septum. The flask was evacuated and backfilled with argon. Toluene (20 mL) and P^{t}Bu$_3$ (8 mL, 0.4 mmol, 0.05 M in toluene) were added. The reaction mixture was heated at 110 °C for 48 h. The reaction mixture was allowed to cool to room temperature, quenched with water (40 mL), and extracted twice with CH_2Cl_2.The combined organic solution was washed with brine and dried over $MgSO_4$. The product was isolated as yellow crystals with recrystallization from methanol to afford **TAM1** (890 mg, 72%). IR (KBr) ν 2959, 1600, 1487, 1368, 811, 745 cm^{-1}; ^{1}H NMR ($CDCl_3$, 400 MHz) δ 8.83 (d, J = 8.0 Hz, 3H), 8.71 (s, 3H), 7.83 (d, J = 8.0 Hz, 3H), 7.69 (d, J = 8.4 Hz, 3H), 7.29 (d, J = 8.0 Hz, 9H), 7.15 (d, J = 8.0 Hz, 15H), 7.10−7.03 (m, 12H), 2.19−2.16 (m, 6H), 2.02−1.99 (m, 6H), 0.46 (t, J = 7.2 Hz, 18H); ^{13}C NMR ($CDCl_3$, 100 MHz) δ 171.4, 152.4, 150.0, 148.0, 147.7, 145.6, 135.5, 134.3, 129.1, 128.4, 124.0, 123.2, 123.0, 122.7, 121.1, 119.0, 118.8, 56.3, 32.7, 8.8; MS (*m*/*z*, FAB$^+$) 1243 (50), 1242 (32), 415 (48), 385 (35), 371 (100); HRMS ((M + H)$^+$, FAB$^+$) Calcd $C_{90}H_{79}N_6$ 1243.6366, found 1243.6379.

TAM2. A procedure similar to that for **TAM1** was applied. A mixture of $Pd(OAc)_2$ (23 mg, 0.1 mmol), biphenyl-4-ylphenylamine (1.0 g, 4 mmol), Na^{t}BuO (460 mg, 6 mmol), **T-Br** (980 mg, 1 mmol), toluene (20 mL), and P^{t}Bu$_3$ (8 mL, 0.4 mmol, 0.05 M in toluene) gave **TAM2** (1.2 g, 82%) as yellow crystals with recrystallization from methanol. IR (KBr) ν 2979, 1607, 1514, 1282, 824, 765 cm^{-1}; ^{1}H NMR ($CDCl_3$, 400 MHz) δ 8.86 (dd, J = 9.2, 1.2 Hz, 3H), 8.74 (d, J = 0.8 Hz, 3H), 7.86 (d, J = 8.0 Hz, 3H), 7.72 (d, J = 8.4 Hz 3H), 7.63−7.61 (m, 6H), 7.53 (d, J = 8.2 Hz, 6H), 7.45 (t, J = 7.6 Hz, 6H), 7.35−7.28 (m, 9H), 7.25−7.19 (m, 15H), 7.15 (dd, J = 10.4 Hz, 2.4 Hz, 3H), 7.08 (t, J = 7.4 Hz, 3H), 2.24−2.19 (m, 6H), 2.06−2.01 (m, 6H), 0.49 (t, J = 7 Hz, 18H); ^{13}C NMR ($CDCl_3$, 100 MHz) δ 171.4, 152.5, 150.0, 147.8, 147.5, 147.0, 145.6, 140.4, 135.7, 135.1, 134.3, 129.2, 128.6, 128.4, 127.7, 126.7, 124.3, 123.8, 123.4, 122.9, 121.2, 119.0, 56.3, 32.8, 8.9; MS (*m*/*z*, FAB$^+$) 1472 (100), 1471 (68), 492 (18), 447 (32), 307 (55); HRMS (M$^+$, FAB$^+$) Calcd $C_{108}H_{90}N_6$ 1470.7227, found 1470.7202.

TAM3. A procedure similar to that for **TAM1** was applied. A mixture of $Pd(OAc)_2$ (23 mg, 0.1 mmol), naphthalen-2-ylphenylamine (900 mg, 4 mmol), Na^{t}BuO (460 mg, 6 mmol), **T-Br** (980 mg, 1 mmol), toluene (20 mL), and P^{t}Bu$_3$ (8 mL, 0.4 mmol, 0.05 M in toluene) gave **TAM3** (700 mg, 53%) as yellow crystals using column chromatography with hexane/toluene (3/1) and then recrystallization from methanol. IR (KBr) ν 2966, 1600, 1520, 1375, 818, 791 cm^{-1}. ^{1}H NMR ($CDCl_3$, 400 MHz) δ 8.81 (dd, J = 9.2, 1.2 Hz, 3H), 8.68 (s, 3H), 7.96 (d, J = 8.4 Hz, 3H), 7.91 (d, J = 8.4 Hz, 3H), 7.81−7.78 (m, 6H), 7.61 (d, J = 8.4 Hz, 6H), 7.48 (m, 6H), 7.38−7.32 (m, 6H), 7.25−7.23 (m, 3H), 7.13−7.11 (m, 9H), 7.01−6.97 (m, 6H), 2.16−2.12 (m, 6H), 1.95−1.89 (m, 6H), 0.41 (t, J = 7.2 Hz, 18H); ^{13}C NMR ($CDCl_3$, 100 MHz) δ 171.4, 152.3, 149.8, 148.8, 148.4, 145.8, 143.5, 135.1, 134.5, 134.0, 130.8, 129.0, 128.3, 126.7, 126.2, 126.1, 125.9, 124.2, 122.9, 122.1, 121.8, 121.1, 119.5, 118.8, 116.4, 56.2, 32.7, 8.8; MS (*m*/*z*, FAB$^+$) 1394 (15), 1393 (12), 460 (16), 307 (100), 289 (45); HRMS ((M + H)$^+$, FAB$^+$) Calcd $C_{102}H_{85}N_6$ 1393.6836, found 1393.6853.

TAM4. A mixture of $Pd(OAc)_2$ (23 mg, 0.1 mmol), carbazole (900 mg, 4 mmol), K_2CO_3 (830 mg, 6 mmol), and **T-Br** (980 mg, 1 mmol) were added to *o*-xylene (20 mL) and P^{t}Bu$_3$ (8 mL, 0.4 mmol, 0.05 M in toluene). The reaction mixture was heated at 160 °C for 5 days. The reaction mixture was allowed to cool to room temperature, quenched with water (40 mL), and extracted twice with CH_2Cl_2.The combined organic solution was washed with brine and dried over $MgSO_4$, and the product was isolated as yellow crystals from column chromatography with hexane/toluene (3/1) and then recrystallized from methanol to afford **TAM4** (630 mg, 51%). IR (KBr) ν 2986, 1620, 1527, 1235, 831, 751 cm^{-1}; ^{1}H NMR ($CDCl_3$, 400 MHz) δ8.98 (dd, J = 9.6, 1.6 Hz, 3H), 8.87 (d, J = 1.2 Hz, 3H), 8.20 (d, J = 7.6 Hz, 6H), 8.07 (t, J = 8.4 Hz, 6H), 7.65−7.63 (m, 6H), 7.49−7.47 (m, 12H), 7.36−7.32 (m, 6H), 2.37−2.33 (m, 6H), 2.24−2.20 (m, 6H), 0.58 (t, J = 7.2 Hz, 18H); ^{13}C NMR ($CDCl_3$, 100 MHz) δ 171.5, 152.9, 150.5, 145.1, 140.8, 139.8, 137.3, 135.3, 128.6, 125.9, 123.3, 121.8, 121.6, 120.3, 119.9, 109.7; MS (*m*/*z*, FAB$^+$) 1238 (20), 1237 (12), 460 (15), 391 (28), 307 (100); HRMS ((M + H)$^+$, FAB$^+$) Calcd $C_{90}H_{73}N_6$ 1237.5897, found 1237.5897.

Characterization. Electrochemical measurements were performed in a conventional electrochemical cell consisting of a working electrode with a ∼1 mm inlaid platinum disk, a Ag wire as a quasireference electrode (referenced verse internal standard, ferrocene/ferrocenium then converting to SCE), and a Pt wire coil as counter electrode. For ECL, the working electrode was a 2 mm platinum disk J-type (bent to face the detector). The working electrode was polished with 1 μm alumina (Buehler, Ltd., IL), and then 0.3 μm and 0.05 μm, followed by sonication in deionized water and acetone for 5 min each. This series of D−A molecules was tested in 1:1 benzene:MeCN, with 0.1 M Bu_4NPF_6 as a supporting electrolyte. Cyclic voltammograms (CVs) were recorded on a model 660 electrochemical workstation (CH Instruments, Austin, TX).

Electrochemical current and ECL transients were simultaneously recorded using an Autolab electrochemical workstation (Eco Chemie, The Netherlands) coupled with a photomultiplier tube (PMT, Hammamatsu R4220p, Japan) held at −750 V with a high-voltage power supply (Kepco, Flushing, NY). The photocurrent produced at the PMT was transformed into a voltage signal by an electrometer/high resistance system (Keithley, Cleveland, OH) and fed into the external input channel of an analog-to-digital converter (ADC) of the Autolab. The ECL spectra were taken using a liquid nitrogen-cooled charge-coupled device (CCD) camera (Princeton Instrument, SPEC-32), which was cooled to −100 °C and calibrated with a mercury lamp. Absorption spectra were recorded with a Milton Roy Spectronic 3000 array spectrophotometer. Fluorescence spectra were acquired on a Quanta Master spectrofluorimeter (Photon Technology International, Birmingham, NJ). Differential scanning calorimetry (DSC) was recorded with JADE DSC (PerkinElmer).

DigiSim 3.03 (Bioanalytical Systems, Inc., West Lafayette, IN) was used to simulate the cyclic voltammograms. The double-layer capacitance (∼40 nF) and uncompensated resistance (1200 Ω) were determined from the current response to a potential step made in a nonfaradic region. The diffusion coefficients, D, were determined from the Randles-Sevic equation and a Cottrell plot of an oxidizing potential step. The electrode surface area was determined from a Cottrell plot of a potential step experiment in 1 mM ferrocene in MeCN ($D = 1.2 \times 10^{-5}$ cm^2/s).[13]

Results and Discussion

Electrochemistry. Cyclic voltammograms for **TAM1**−**TAM4** are shown in Figure 2, and Table 1 summarizes the electrochemical results. All **TAM** compounds show one reversible reduction peak at (1 to 4) −1.79, −1.78, −1.78, and −1.74 V vs SCE, respectively. The reduction peaks were reversible even at a slow scan rate (50 mV/s), indicating a long-lived radical anion. The radical anion is reasonably assigned the 1,3,5-triazine (A) core and is relatively insensitive to the substituent groups. The reduction peak potential separation between the forward scan and reverse scan was ∼65 mV at 100 mV/s, slightly greater than ∼58 mV expected for a one-electron process.[14] The additional 6 mV is attributed to *i*R drop in the highly resistive solvent, so the reduction is believed to be a single electron transfer. Moreover, the same peak splitting was observed for the reference material, ferrocene, which is known to undergo one-electron oxidation. Digital simulation of reduction CV at different scan rates was performed to confirm the reduction mechanism (Supporting Information, Figure S3). The best fit between the experimental and simulated CVs was observed from 50 mV/s to 1 V/s, assuming the reduction mechanism is a simple electron transfer with no coupled homogeneous chemical reactions. The best fit was obtained, after correction for R_u, a heterogeneous electron transfer rate constant, $k^o \sim 0.02$ cm/s. This relatively slow electron transfer for a simple outer sphere reaction might be caused by a large conformational change in the molecule upon reduction.

(8) For review on ECL: (a) Bard, A. J. *Electrogenerated Chemiluminescence*; Marcel Dekker: New York, 2004. (b) Miao, W. *Chem. Rev.* **2008**, *108*, 2506. (c) Knight, A. W.; Greenway, G. M. *Analyst* **1994**, *119*, 879. (d) Richter, M. M. *Chem. Rev.* **2004**, *104*, 3003.
(9) (a) Lai, R. Y.; Fabrizio, E. F.; Jenekhe, S. A.; Bard, A. J. *J. Am. Chem. Soc.* **2001**, *123*, 9112. (b) Rashidnadimi, S.; Hung, T.-H.; Wong, K.-T.; Bard, A. J. *J. Am. Chem. Soc.* **2008**, *130*, 634.
(10) Chandross, E.; Sonntag, F. *J. Am. Chem. Soc.* **1966**, *88*, 1089.
(11) Reichardt, C. *Solvents and Solvent Effect in Organic Chemistry*; Wiley-VCH Verlag GmbH & Co. KGaA: Weinheim, Germany, 2003.
(12) Saroja, G.; Pingzhu, Z.; Ernsting, N. P.; Liebscher, J. *J. Org. Chem.* **2004**, *69*, 987.
(13) Kadish, K.; Ding, J.; Malinski, T. *Anal. Chem.* **1984**, *56*, 1741.
(14) The exact difference in the peak potentials for a nernstian reaction with no resistive effects depends slightly on the potential for scan reversal past the wave of interest. Bard, A. J.; Faulkner, L. R. *Electrochemical Methods*; Wiley: New York, 2001, p 242.

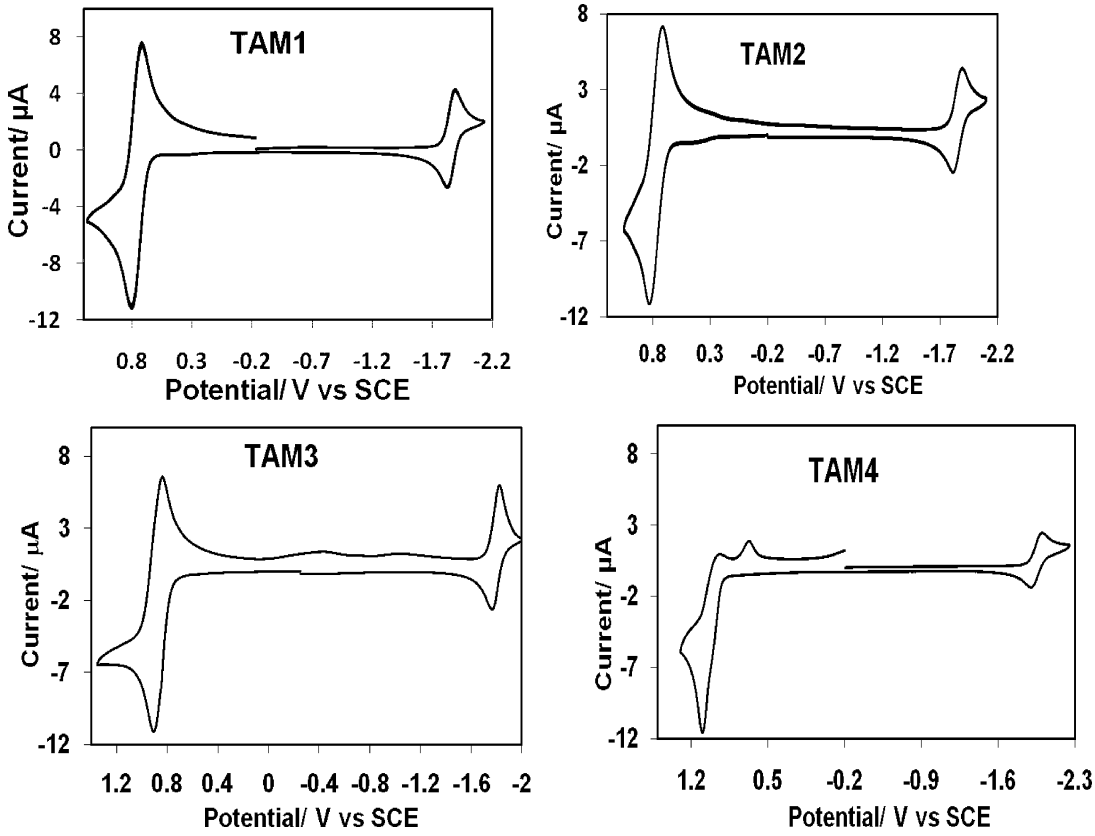

Figure 2. Cyclic voltammograms of **TAM1**−**TAM4** in 1:1 Bz:MeCN, 0.1 M Bu_4NPF_6, scan rates 100 mV/s. Working electrode: Pt inlaid disk (diameter ~ 0.5 mm), counter electrode: Pt coil, reference electrode: Ag QRE.

Table 1. Electrochemical Results[a]

	oxidation potential $E_{1/2}^{oxd}$ (V)	reduction potentials $E_{1/2}^{red1}$ (V)	D (cm^2/s)	HOMO[b] (eV)	LUMO[b] (eV)	E_g (eV)
TAM1	0.81	−1.79,	4×10^{-6}	−5.27	−2.67	2.60
TAM2	0.82	−1.78,	5×10^{-6}	−5.27	−2.67	2.60
TAM3	0.85	−1.78,	5×10^{-6}	−5.23	−2.67	2.80
TAM4	1.18	−1.74,	3×10^{-6}	−5.63	−2.71	2.92
PTAM4	0.93	−				
	1.15					

[a] All potentials are versus SCE. [b] HOMO $= -E^{ox}{}_{vs\ Fc/Fc+} - 4.8$ eV. LUMO $= E_g -$ HOMO. $E_g = E^{ox} + E^{red}$.

TAM1−**TAM3** show chemically reversible oxidation peaks at 0.81, 0.82, 0.82 V vs SCE, respectively (Figure 1). The magnitude of anodic peak current ($i_{pa} \sim 12\ \mu$A) was three times that of the cathodic peak current ($i_{pc} \sim 4\ \mu$A), suggesting that the oxidation process is an overall three-electron transfer process and attributed to the oxidation of each donor group essentially simultaneously. The CV simulation results (Supporting Information, Figure S4) suggest three sequential electron transfers with the ΔE^o between each wave of 20−40 mV, with $D_o = 6 \times 10^{-6}$ cm^2/s and with a fast heterogeneous rate constant (simulation $k^o = 1 \times 10^4$ cm/s), e.g., nernstian reactions. That the three donor groups oxidize at very nearly the same potential suggests lack of electronic communication among the D groups (diarylamino), implying the triazene core and the fluorene linkers serve as good electron delocalization blocking groups. However, the fact that the peak splitting is larger than ~58 mV suggests that there is some interaction, perhaps electrostatic.[15] The electrogenerated trication was stable at scan rates as low as 50 mV/s; even after 100 cycles there was no evidence of decomposition or dimer formation.

TAM4 is oxidized at 1.18 V, which is considerably more positive than the potential for oxidation of the diarylamino-capped species. However, the radical cation is unstable, so that the reverse wave is much smaller than for the other **TAM** compounds, and a new reduction wave of a product appears on the reverse scan. This could be a dimer that forms through the coupling of the two carbazole units at the C3 or C6 position (and, as described in the next section, some polymer).[16] The dimer can be electrochemically oxidized more easily, at 0.88 V (Figure 3). Scheme 3 shows a possible, but still speculative, mechanism for the formation of a dimeric compound from the two bulky, star-shaped carbazole molecules. However, the first oxidation of carbazole is a mixture of ECE and EC mechanisms, in which the following chemical reaction is very fast.[17,6b] That means the oxidation of carbazole after the first cycle is an ECE mechanism (Scheme 3).[17] Continuous cycling leads to an increasing growth of the smaller oxidation peak, which indicates a polymer film is formed on the surface of the electrode, consistent with previous studies of a related species.[18]

PTAM4 (Polymer of TAM4). TAM4 can electropolymerize to give a coating on the surface of the electrode.[16] After 10 cycle scans (scanning first to the oxidation potential of the

(15) Flanagan, J. B.; Margel, S.; Bard, A. J.; Anson, F. C. *J. Am. Chem. Soc.* **1978**, *100*, 4248.

(16) (a) Marrec, P.; Dano, C.; Simonet, N. G.; Simonet, J. *Synth. Met.* **1997**, *89*, 171. (b) Abe, S. Y.; Bernede, J. C.; Delvalle, M. A.; Tregouet, Y.; Ragot, F.; Diaz, F. R.; Lefrant, S. *Synth. Met.* **2002**, *126*, 1. (c) Inzelt, G. *J. Solid State Electrochem.* **2003**, *7*, 503.

(17) (a) Ambrose, J. F.; Nelson, R. F. *J. Electrochem. Soc.* **1968**, *115*, 1159. (b) Ambrose, J. F.; Carpenter, L. L.; Nelson, R. F. *J. Electrochem. Soc.* **1975**, *122*, 876.

(18) Natera, J.; Otero, L.; Sereno, L.; Fungo, F.; Wang, N.-S.; Tsai, Y.-M.; Hwu, T.-Y.; Wong, K.-T. *Macromolecules* **2007**, *40*, 4456–4463.

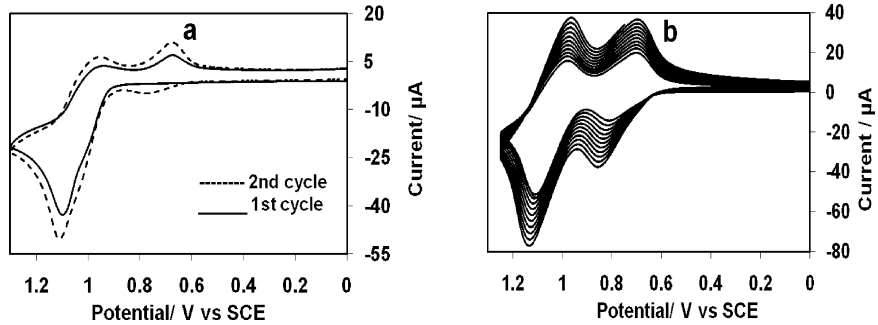

Figure 3. Cyclic voltammograms of 1 mM **TAM4** in dry acetonitrile, 0.1 M Bu_4NPF_6. Working electrode: Pt inlaid disk (diameter ~ 2 mm), counter electrode: Pt coil, reference electrode: Ag QRE. (a) Comparison between first and second cycle. (b) After 10 cycles.

Scheme 3. Electrooxidation of **TAM4** and the Following Dimerization Reaction

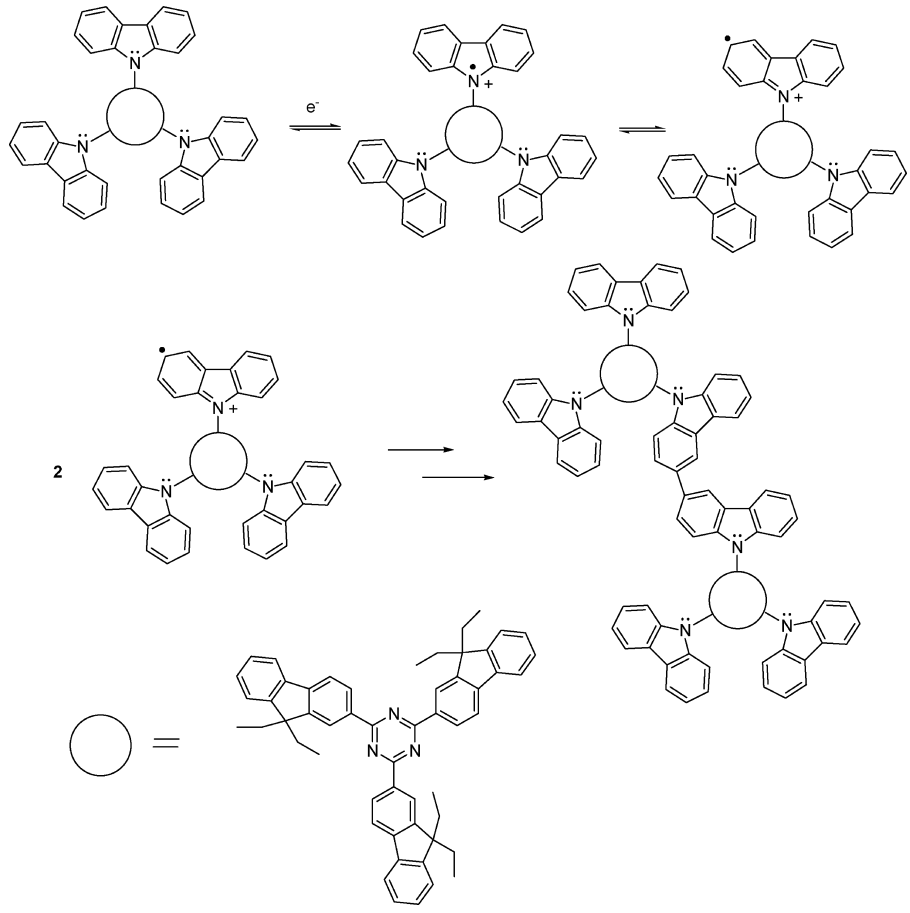

monomer of **TAM4**), an orange thin film could be seen to build up on the surface of the working electrode during this cycling. Both the original wave seen on the first scan, and the second that builds up at less positive potentials, increased with the number of scans. This suggests the formation of an electroactive and conducting polymer upon oxidation of **TAM4** (Figure 3a and 3b). The working electrode coated with **PTAM4** was washed with the same solvent, dried in air, and then placed in a fresh electrolyte solution without monomer. The new polymer-modified electrode produced two distinct and reversible oxidation peaks, the first at 0.93 V and the second at 1.15 V vs SCE (Figure 4a). The scan rate dependence of the polymer film (Figure 4b) shows a peak current directly proportional to the scan rate at low scan rates, which deviates from this trend at scan rates above about 0.3 V/s, suggesting kinetic limitations in the oxidation, perhaps associated with bringing counteranions into the film. The **PTAM4** shows electrochromic behavior and is pale orange in the neutral state, changing to dark green when it is oxidized. The **PTAM4** electrochromic behavior was stable for at least 2000 cycles, suggesting the possibility of applications.

A question of interest is why the radical cation of the carbazole-substituted species, **TAM-4** undergoes rapid dimerization, while those of the diarylamine-substituted ones, **TAM1**−**TAM3**, do not. Related parent compounds, e.g., triphenylamines and carbazoles, have been studied by Adams, Nelson, and co-workers,[6,17] While the simple parent triphenylamine dimerizes rapidly, the rate of dimerization depends strongly on the nature of para-substitution; for example, monosubstituted *p*-tolyldiphenylamine is much more stable than the parent, and radical cation of tri*p*-tolylamine is very stable.[17] Thus, the effective para-substitution by the fluorene and triazine as well as the considerably increased steric hindrance together

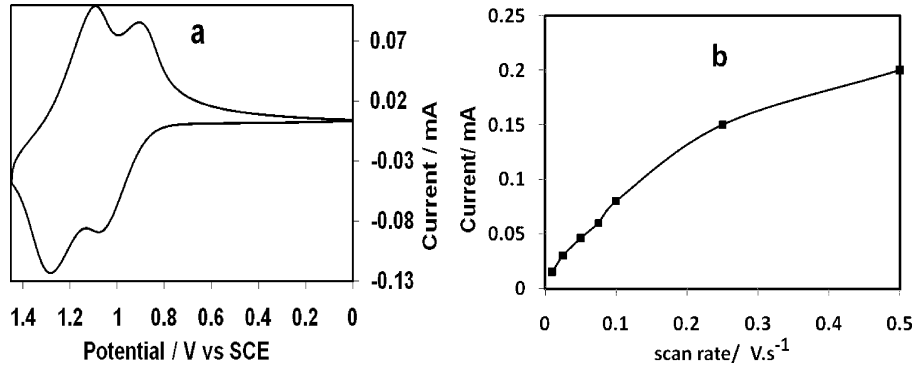

Figure 4. **PTAM4** on Pt electrode in MeCN, 0.1 M Bu_4NPF_6. (a) Anodic oxidation of **PTAM4**, scan rate: 100 mV/s. (b) Scan rate dependence of the polymer film oxidation from 10 mV/s to 500 mV/s.

act to stabilize the radical cations, even for the more highly oxidized states. The carbazolium radical cations, even substituted ones, are less stable.[17,18]

The substituents affect the energy of the highest occupied molecular orbital (HOMO) as derived from the half wave peak potentials, taking the energy of the HOMO $= -E^{ox}_{vs\ Fc/Fc+} - 4.8$ eV.[19] From the results in Table 1, for the star-shaped D−A molecules (**TAM1**−**TAM3**) with diarylamino end-capping groups, the frontier energy levels are similar but very different from that of carbazole-containing compound (**TAM4**). This result is strongly related to the relative electron-donating abilities of the diarylamino groups and carbazole (that can be considered to be a radical cation localized inside the carbazole ring because of its coplanar structure.) The lowest unoccupied molecular orbital (LUMO) is the about the same for **TAM1**−**TAM4** since reduction mainly involves the triazine group in all of these.

Photophysical Properties. Absorption and fluorescence spectra of the **TAM** compounds were taken in the same solvent as used for electrochemistry and ECL experiments (1:1 MeCN:benzene). The spectra are shown in Figure 5a and 5b, respectively. Table 2 summarizes the photophysical properties of **TAM1**−**TAM4**. The absorption spectra of **TAM1**−**TAM3** are very similar and gave λ_{max} centered at ca. 420 nm, while **TAM4** shows a λ_{max} at 370 nm. Similarly (Figure 5b) **TAM1**−**TAM3** gave emission maxima at about the same λ_{max} centered at 565 nm, showing that the different substituent groups have only a small effect on electron-donating ability toward the triazene core. In contrast, **TAM4** gave an emission maximum centered at 505 nm, blue-shifted from the others by 60 nm due to the weaker electron-donating ability of carbazole. These results agree with the electrochemical results, showing that diarylamino end-capping groups extend the π-conjugation along the fluorene bridge to the central triazene better than that of the carbazole. The PL quantum yields of **TAM1**−**TAM4** were estimated using rubrene as a standard. For **TAM1**−**TAM3**, these were ∼80% in 1:1 Bz:MeCN, while that of **TAM4** was about 70% in the same solvent.

These D−A molecules show large solvatochromic effects in the emission, while the absorption spectra are independent of solvent polarity. A small Stokes shift is observed in less polar solvents such as hexane ($\lambda_{max,PL} = 428$ nm), while a large Stokes shift is observed in polar solvents such as DMF ($\lambda_{max,PL} = 575$ nm), as shown in Figure 5c−e. Additionally, the intensities of PL emission decrease with increasing solvent polarity, a strong indication of the polar character in the excited states. Therefore, the **TAM** compounds have strong electronic interactions between the donor and acceptor subunits in the excited state but weak ones in the ground state. This solvatochromism indicates that the stabilization of the excited state is larger than that of ground state by the surrounding solvent molecules.[20]

Electrogenerated Chemiluminescence (ECL). The **TAM** compounds (except for **TAM4**) are good candidates for ECL generation, because they show high PL quantum yields and exhibit stable radical ion species, as shown in the cyclic voltammograms. Figure 6 displays the ECL spectra of these molecules. In the simple ECL mechanism, light is produced during annihilation between the cation radical and the anion radical. However, for these D−A molecules, the annihilation can also occur between the anion radical and the radical bi- and trication species.

TAM1−**TAM3** give relatively strong ECL, which could be seen by the naked eye in a well-lit room. Figure 6 shows the ECL spectra, which are similar to their fluorescence spectra, showing that the emission is mainly from the excited monomer. The very small red-shift of the ECL spectra relative to the PL spectra normally encountered in ECL studies is attributed to an inner filter effect owing to the high sample concentration used for ECL and also to a small instrumental offset. The ECL spectrum of **TAM2** taken with a dilute solution (0.2 μM), the same as that used in the PL, was obtained with the same CCD detector used for ECL experiments, showed that emission shifted by only 3 nm. The ECL probably occurs via the S-route, since the enthalpy of annihilation ($\Delta H_{ann} = E_{1/2}{}^{ox} - E_{1/2}{}^{red} - 0.1$) is larger than the energy required to generate the excited singlet state E_s. In contrast, **TAM4** shows only a very weak and broad ECL peak (Figure 7). The weak ECL emission of **TAM4** is ascribed to instability of the radical cation and the formation of the polymer film on the electrode surface. The broad emission band (bandwidth ∼ 330 nm) might indicate ECL emission by the dimer formed during the electrolysis. However, when benzoyl peroxide (BPO) was used as a coreactant with only reduction, a strong ECL peak was observed (Figure 6d) with the coreactant-induced ECL spectrum of **TAM4** narrower and similar to the PL spectrum. This suggests that the annihilation ECL of **TAM4** (i.e., pulsing from E_{pa} + 80 mV to E_{pc} − 80 mV) is mainly due to the emission of the monomer, dimer, and perhaps the polymer. We attempted to obtain the ECL spectrum of an electrochemically produced polymer film (**PTAM4**) in a monomer-free solution with and without coreactant. Although the emission was too weak to obtain an ECL spectrum with a

(19) (a) Li, Y.; Cao, Y.; Gao, J.; Wang, D.; Yu, G.; Heeger, A. J. *Synth. Met.* **1999**, *99*, 243. (b) Gritzner, G.; Kuta, J. *Pure Appl. Chem.* **1984**, *56*, 462.

(20) Brunel, J.; Mongin, O.; Jutand, A.; Ledoux, I.; Zyss, J.; Blanchard-Desce, M. *Chem. Mater.* **2003**, *15*, 4139.

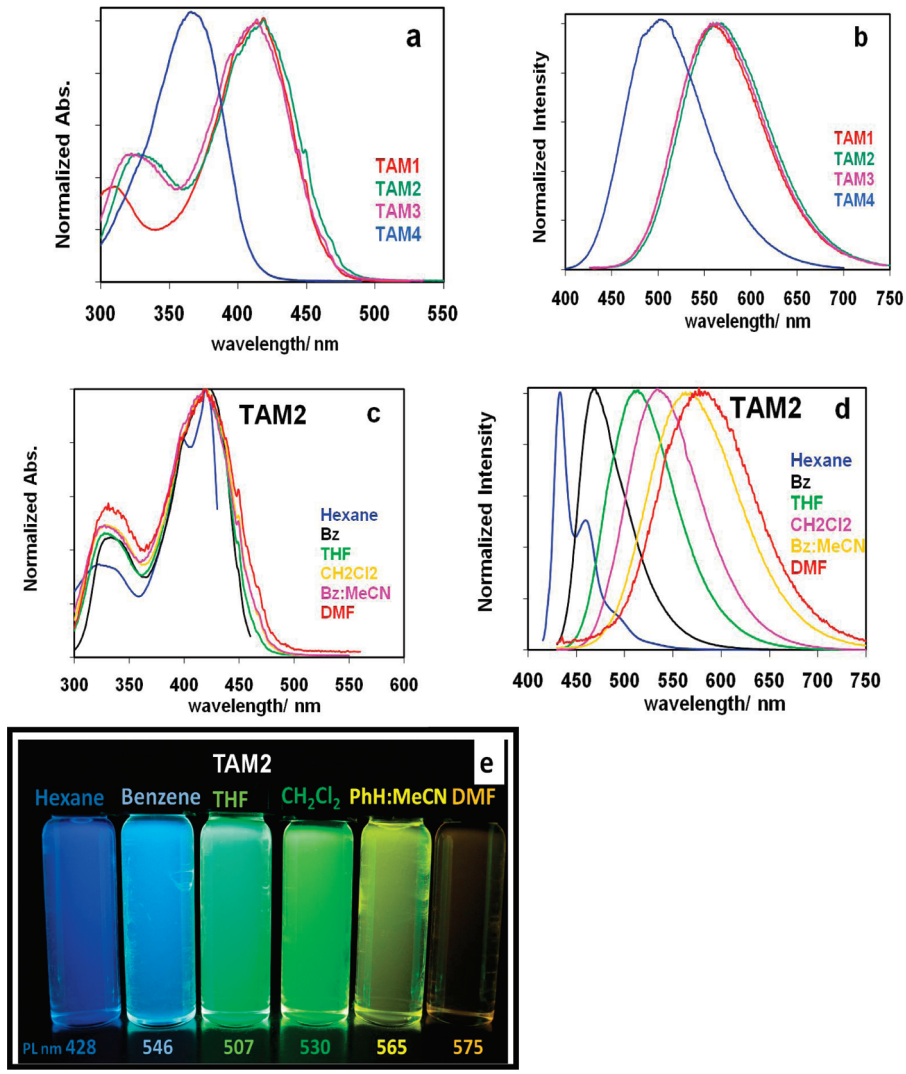

Figure 5. (a) Absorption spectra of **TAM**s in 1:1 MeCN:Bz. (b) Fluorescence spectra. (c) Absorption spectra of **TAM2** in different solvents as indicated in the figure. (d) Fluorescence spectra of **TAM2** in different solvents as indicated in the figure. Absorption and emission spectra are normalized. (e) Picture of **TAM2** in different solvents with PL maxima in each solvent shown.

Table 2. Spectroscopic and ECL Results of **TAM1**−**TAM4** in 1:1 MeCN:Bz

	λ^{Abs}_{max}	λ^{PL}_{max}	$\lambda_{max,ECL}$ (nm)	E_s (eV)[a]	ΔH^o_{ann}	$\Phi^{PL\,b}$	$\Phi^{ECL\,c}$
TAM1	418	562	574	2.20	2.50	0.81	0.5
TAM2	418	565	575	2.19	2.50	0.85	0.5
TAM3	418	562	575	2.20	2.50	0.81	0.5
TAM4	370	505	518	2.45	2.72	0.70	–

[a] $E_s = 1239.85/\lambda_{max}{}^{PL}$. [b] Compared to rubrene. [c] Relative to the ECL of DPA taking Φ^{ECL} (DPA) as 1.

CCD, with a more sensitive photomultiplier tube (PMT) as a detector, ECL light from the polymer could be recorded; we did not attempt to obtain a spectrum with band-pass filters.

Figure 8 shows the profile of **TAM2** ECL intensity versus time for individual potential steps. The alternation of potential was pulsing from E_{pa} + 100 mV to E_{pc} − 100 mV, which is sufficient to oxidize and reduce **TAM2**. Unlike the usual profiles from annihilation of stable radical monoions, where equal emission is found on anodic and cathodic steps, the ECL emission here shows much larger emission in the reduction steps (Figure 8). This behavior was independent of the direction of the first potential step. The difference here is that the annihilation reaction involves the trication reacting with the monoanion. This involves several different routes, such as

$$D^{3+\bullet} + D^{\bullet-} \rightarrow D^* + D^{2+\bullet} \quad (14)$$

along with various comproportionation reactions, e.g.,

$$D^{3+\bullet} + D \rightarrow D^{+\bullet} + D^{2+\bullet} \quad (15)$$

followed by radical annihilation. In work to be published elsewhere, we have shown through digital simulation that such behavior is expected when there are significant differences in the concentrations of oxidizing and reducing equivalents. In this case, the availability of a higher concentration of one of the reactants diffusing away from the annihilation zone and back during the following pulse will lead to a larger emission and a more extended transient decay, in this case occurring during the cathodic pulse when the trication formed upon oxidation reacts with the anion.

Conclusion

A series of highly fluorescent, star-shaped donor−acceptor molecules with an electron-accepting triazine core bridged by fluorene linked to electron-donating diarylamino and carbazolyl

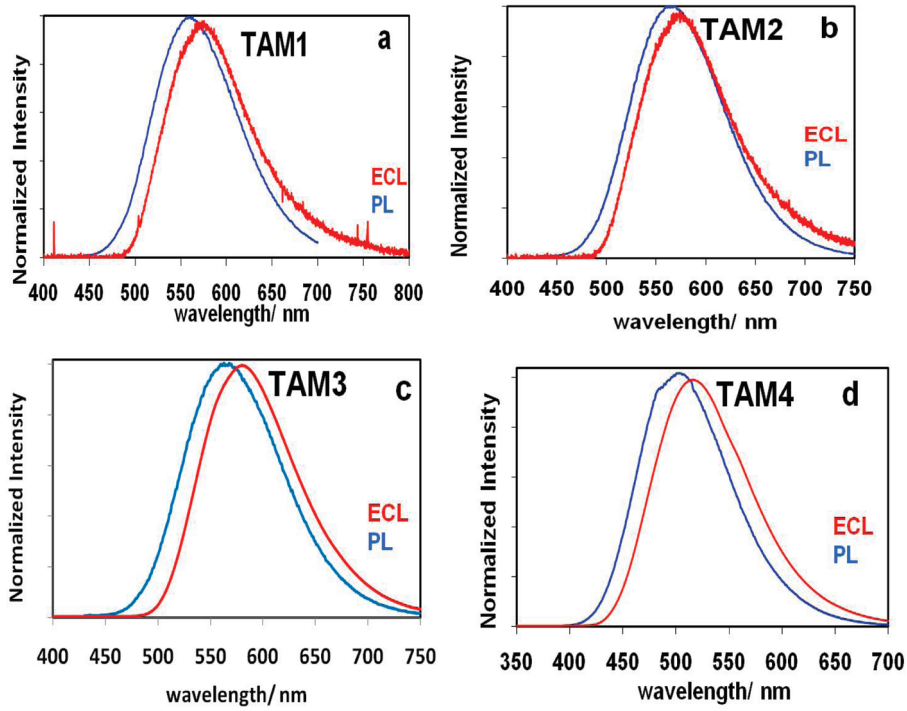

Figure 6. ECL and PL spectra for the 1 mM star-shaped molecules in 1:1 MeCN:Bz, 0.1 M Bu_4NPF_6 as a supporting electrolyte. **TAM1**−**TAM3** are direct annihilation ECL (E_{pc} − 80 mV and E_{pa} + 80 mV). **TAM4** is coreactant ECL using 10 mM BPO. WE is J-type ~ 2 mm platinum electrode, RE is Ag wire as a quasireference electrode, CE is Pt coil.

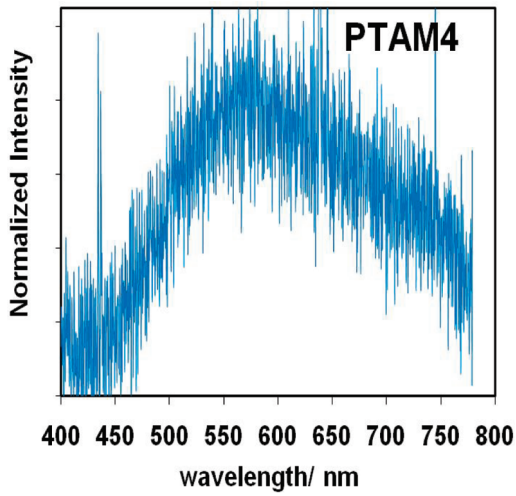

Figure 7. ECL spectrum of **TAM4**, by direct annihilation. Applied potential pulsed between the reduction potential (E_{pc} − 80 mV and E_{pa} + 80 mV) of the dimer formed on the oxidation side.

groups were synthesized and characterized. The donor−acceptor configuration produces a strong photoinduced charge separation in the excited state, and strong solvatochromism in the PL spectra. The electrochemical oxidation of the triarylamino terminus of **TAM1**−**TAM3** gave rise to stable radical trications, whereas a stable radical anion was formed upon the reduction of the triazene core. Dimerization of the carbazole-substituted **TAM4** was observed during the electrochemical oxidation, producing a polymer film on the electrode surface. The polymer film (**PTAM4**) exhibits electrochromic behavior: pale orange in the neutral state and dark green in oxidized state.

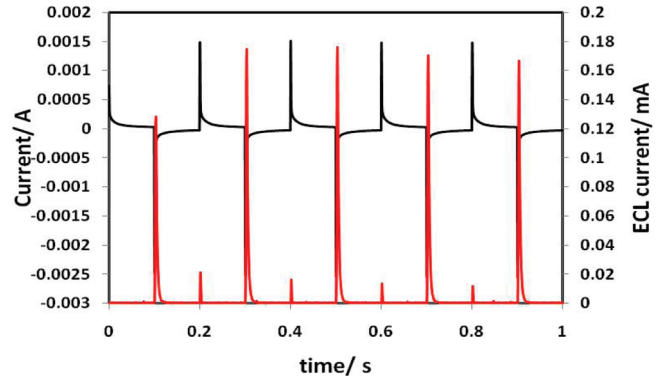

Figure 8. i−t curve for **TAM2**, pulse time: 0.1 s, step pattern: E_{pa} + 100 mV to E_{pc} −100 mV vs SCE. ECL photocurrent (red line); electrochemical current (black line). Anodic pulse is positive; cathodic pulse is negative.

TAM1−**TAM3** show relatively strong ECL, while **TAM4** only shows weak ECL via the direct annihilation reaction. However with BPO as a coreactant, bypassing the electrochemical oxidation step, **TAM4** produced strong ECL.

Acknowledgment. We thank Roche, Inc. and the Robert A. Welch Foundation (F-0021) for support of this research. We also thank the National Science Council of Taiwan for financial support.

Supporting Information Available: Text giving additional synthesis information for **TAM1**−**TAM4**; figure showing the numbering of the carbons in **TAM1**−**TAM4**. This material is available free of charge via the Internet at http://pubs.acs.org.

JA104160F